Proceedings of the 7th International Conference on Asian and Pacific Coasts (APAC 2013) Bali, Indonesia, September 24-26, 2013

A STUDY ON THE LONGSHORE SEDIMENT TRANSPORT RATE AROUND A HEADLAND

S. An [1] and S. Takewaka [2]

ABSTRACT: This study tries to estimate the variation of longshore sediment transport rates (LSTR) around a jetty, or a headland, from observational data and numerical computation. X-band radar was installed to observe hourly waves and morphology around the headland at Kashima Coast, Ibaraki, Japan. Several features, such as the surfzone, shoreline positions, and wave crest locations, are digitized from the radar images. Then the intertidal beach slopes were evaluated with shoreline positions and tidal records. Incident wave height, period, and direction were measured at NOWPHAS wave station at Kashima Port with 2 hours interval. Annual variation of shoreline position, intertidal slope, and incident wave height and direction are summarized to analyze LSTR in the vicinity of the headland. Annual variations of the shoreline positions and the intertidal slopes were analyzed at the northern and southern sides of the headland. Northern sides of the headland are generally accumulating in winter season and are eroding in summer season, and at the southern side, the opposite is observed. These features are corresponding to seasonal wave characteristics. Incident wave directions are primary from the northern; to the headland in winter season and from southern in summer season. From the shoreline positions and the intertidal slopes, cross sectional areas and beach volumes are estimated, and then LSTR are evaluated from change rates of beach volumes. To compute LSTR, wave and current fields were computed for every 2 hours. The numerical results are verified by comparing widths of the surfzone and wave directions read from radar images. Wave breaking height, widths of the surfzone and current speeds from the numerical computation are used to estimate LSTR with several formulas. For the period with fair wave climate, reasonable agreement is obtained for LSTR estimation between observation and computation.

Keywords: Longshore sediment rates, headland, x-band radar, Kashima, numerical computation

INTRODUCTION

In order to solve a considerable number of problems related with coastal engineering by erosion and accumulation caused by longshore sediment transport, many researches for an estimation of longshore sediment transport rate (LSTR) have been studied.

Main objectives of this study are estimations of the LSTR in the vicinity of artificial constructions such as headland and jetty form observational data and numerical computation. The study site is a headland located at Kashima coast, Ibaraki, Japan.

Around the headland, X-band radar is installed to trace hourly waves and morphology change in the vicinity of the headland. By data processing of results from the radar, annual shoreline positions, intertidal beach slopes, beach volumes, and LSTR around the headland are estimated and discussed. With a numerical model, LSTR is computed and compared with observational results.

STUDY SITE & DATA PROCESSING

Study Site

Fig.1 is an aerial photograph of the study area. The study area is approximately 3.8 km south form the research pier HORS, PARI (http://www.pari.go.jp). We define a local coordinate system, and the headland located at X=0 m. The X-band radar (Fig. 2) is installed at (X, Y) = (120 m, 0 m) to trace the hourly wave's circumstances and waterline distribution around the headland. From results of radar measurements, significant features, such as the surfzone, waterline position and wave crest locations, are digitized from.

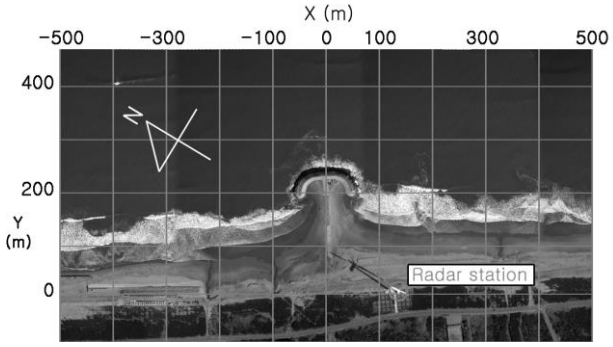

Fig.1 Coordinate system of the study site

[1] Graduate School of System and Information Engineering, University of Tsukuba, 305-5873 JAPAN
[2] Division of Engineering Mechanics and Energy, University of Tsukuba, 305-5873 JAPAN

Fig.2 X-band radar installed at the study site

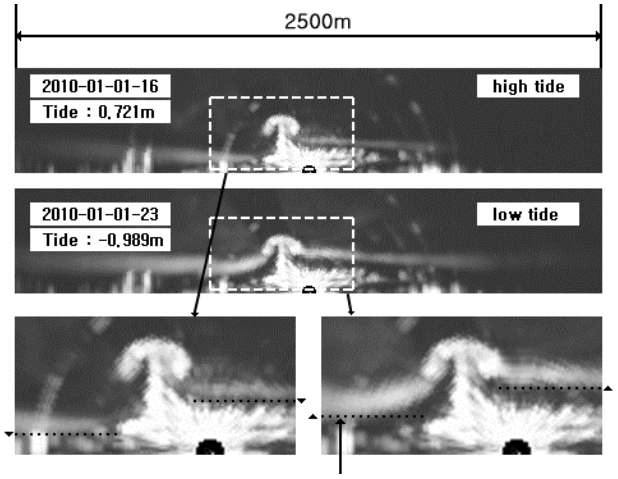

Fig. 3 Time averaged images around headland off shore shift of shoreline position due to ebb tide

Data processing

Radar data are collected and processed every hour to time averaged images (Takewaka, 2005). Data collected for year 2010 are analyzed in this study. Fig. 3 shows time averaged images for high and low tide. It shows that shoreline positions shift seawards by ebb tide (black dotted lines of bottom panel in Fig. 3).

Six locations, X=-200 m, -150m, -100 m, 100 m, 150m, and 200 m in Fig. 1, are selected to process time-stack images to estimate shoreline position, intertidal slope, and cross sectional area. Fig. 4 is a part of time-stack image for 15 days, which shows hourly instantaneous shoreline positions of X=-100 m and X=100 m with tidal variation.

Time-stack image shows variation of shoreline position in time. White lines in the top and mid panel are shoreline positions marked by manual inspection and bottom panel shows the measured tidal variation. Fig. 4 shows that shoreline moves seaward when the tide is ebbing and vice versa in tidal cycle.

Variation of shoreline positions, intertidal beach slopes, cross sectional areas, and beach volumes are estimated in the following manner: Intertidal beach slopes are calculated by using linear regression method with the measured shoreline position and tide (Fig. 5). Data length used for the regression is 7 days. Mean shoreline position is defined at crossing between mean water level and fitting line as shown in Fig. 5. Cross sectional area is also estimated from the result of regression for the height from 0.0 m to -0.7 m around mean sea level (Fig. 6). Beach volumes are then calculated with the averaged cross sectional areas of both sides of the headland and distance between measurement locations.

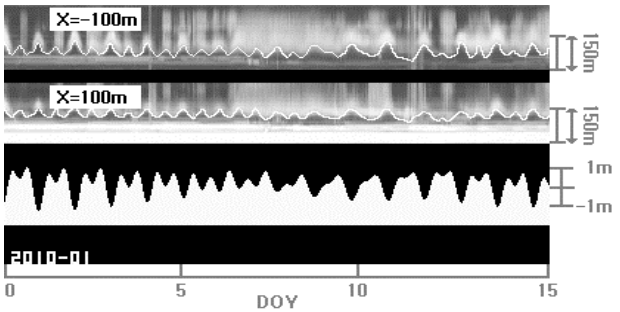

Fig.4 Time stack for X=-100 m and X=100 m, and tide level (bottom panel) for period of day 0 to 15 (DOY, 2010)

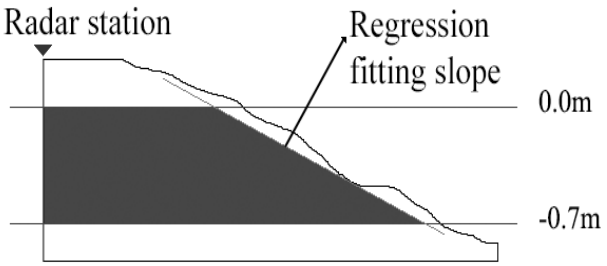

Fig. 5 Regression of instantaneous shore position and definition of the shoreline

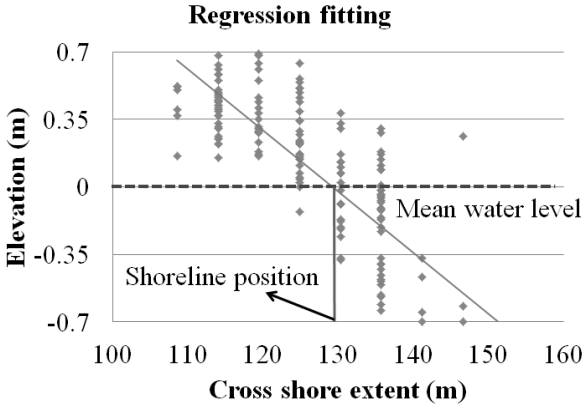

Fig. 6 Sketch of the cross profile with fitting slope

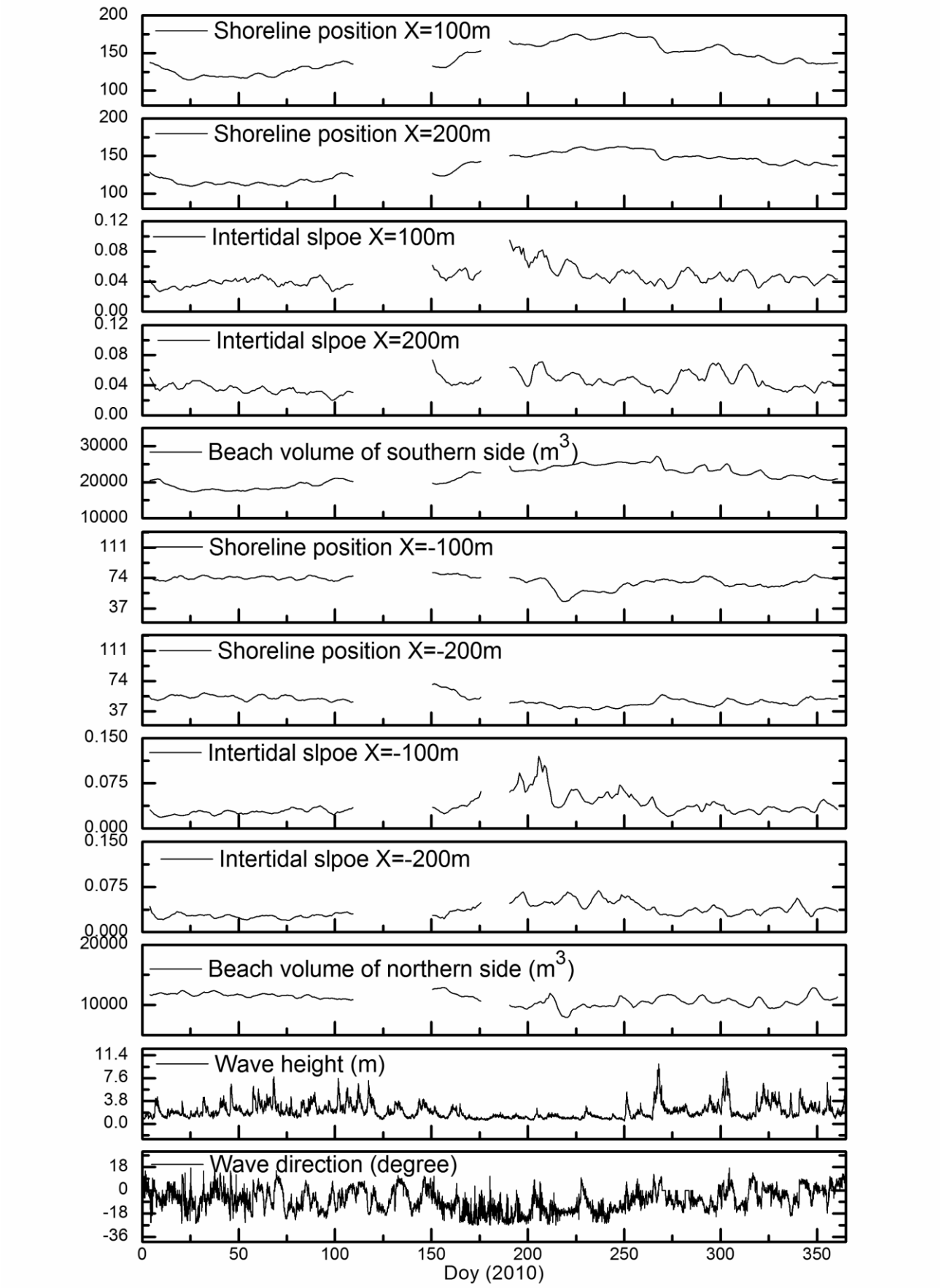

Fig.7 Annual variation of shoreline position, intertidal slope, beach volume, wave height and direction of year 2010.

Result of Data processing

Fig. 7 shows annual variation of shoreline position, intertidal beach slope, beach volume, and significant wave height and wave direction measured at Kashima Port. Positive wave direction indicates northern incident wave, and 0° indicates normal incidence to shore.

Wave characteristics are different with seasons: In winter season, wave heights are high and higher incident waves arrive from the northern. On the other hand, in summer season, wave heights are low and primary incident wave direction is southern.

Shoreline positions are fluctuating all the year. Northern sides (X=-200 m, and X=-100 m) of the headland are generally accumulating in winter season and are eroding in summer season. Southern sides (X=100 m and X=200 m) of the headland have the opposite trend.

Seasonal changes of shoreline positions shown in Fig. 7 are corresponding to seasonal wave characteristics. In summer season, waves are arrived from southern. Therefore, sediments are travelling from south to north, so southern sides of the headland are accumulating, and northern sides of the headland are eroding. Contrary situations occur on account of northern incident waves for winter season.

From the intertidal beach slopes, although trends of variation on the intertidal beach slope are slightly complex, it can be recognized that variations of the intertidal beach slopes are corresponding to advance and retreat of shoreline position. For the period of day of year (DOY) 150 to 175, when northern sides of the headland are eroding, the intertidal beach slopes are becoming steeper. On the other hand, when southern sides of the headland are accumulating, DOY 150 to 175, the intertidal beach slopes are becoming milder.

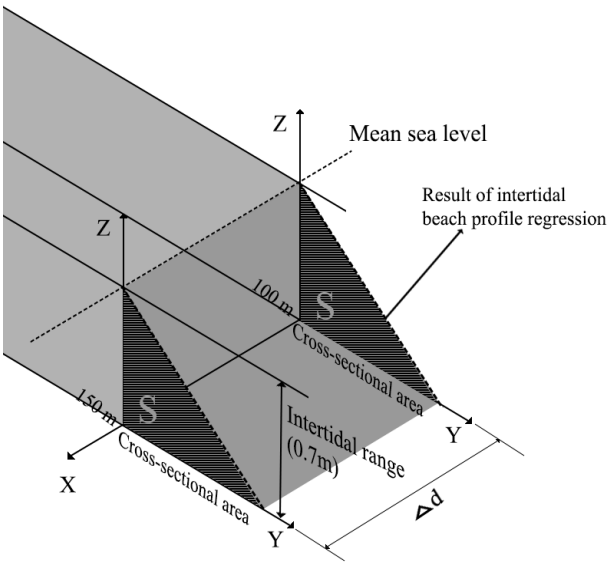

Fig.9 Estimation of the intertidal beach volume

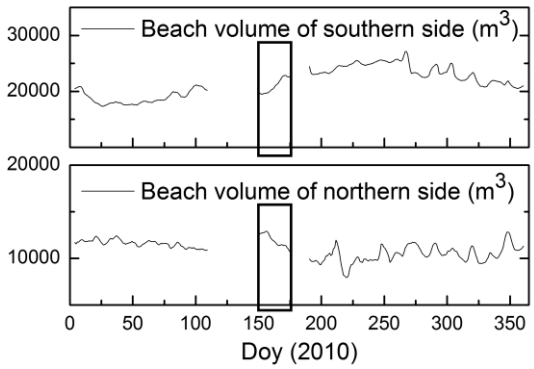

(a) Annual variation of beach volumes

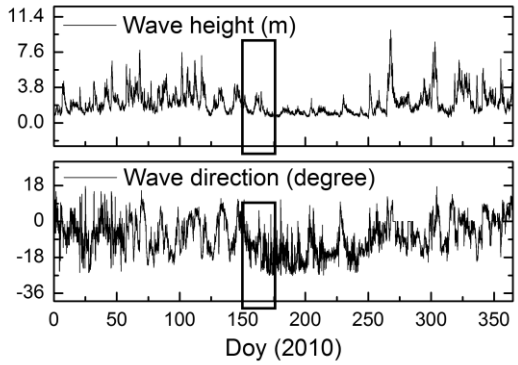

(b) Annual variation of wave height and wave angle

Fig.8 Annual variation of beach volumes and wave conditions of year 2010

As shown in Fig. 6, cross-sectional area of the shore is estimated, and then by multiplying distances between selected location (X=-200 m, -150 m, 100 m, 100 m, 150 m, and 200 m), beach volumes in the intertidal range are estimated. The estimated beach volumes could be used as indexes determining occurrence of erosion or accumulation, and LSTR could be calculated form the change rate of beach volumes.

ESTIMATIONS ON THE LSTR

In this section, a numerical model is applied to estimate LSTR around of the headland for a specific period. The specific period is from DOY 150 to 175 (around 1 month), and it can be seen from Fig. 8 (b) that wave heights of this period generally moderate and primary incident wave directions are from southern, hence, we regard the variation proceeded in almost constant manner . As shown in Fig. 8 (a), northern side of the headland is eroding for this p, whereas, southern side of the headland are accumulating for this section.

Estimation on the LSTR from Radar Observation

To estimate the LSTR from radar measurement, variations of beach volumes are estimated by multiplying cross-sectional area and distance between locations as described in the previous chapter. The concept is shown in Fig. 9, which shows the segment

from X=100 m to 150 m. In Fig. 9, X is alongshore direction, Y is cross-shore direction, and Z is height of shore. S is cross-sectional area sketched in Fig. 6. Intertidal range is 0.7m, the height from 0.0 m to -0.7 m around mean sea level, and Δd (=50 m) is the distance cross section. Beach volume segment for this section is estimated by $S \times \Delta d$.

Through these processes, beach volumes for each segments (X= -200 m ~ -150m, -150 m ~ -100 m, -100 m ~ 0 m, 0 m ~ 100 m, 100 m ~ 150 m, and 150 m ~ 200 m) are calculated and then are summed up for northern and southern side of the headland. Fig. 10 shows variations of beach volumes at northern and southern side of the headland for test period (DOY 150 ~ 175), and monthly-averaged LSTR could be simply estimated by ratio of change of variation graph. Monthly-averaged LSTR of northern side is 89[m^3/day] and of southern side is 162[m^3/day].

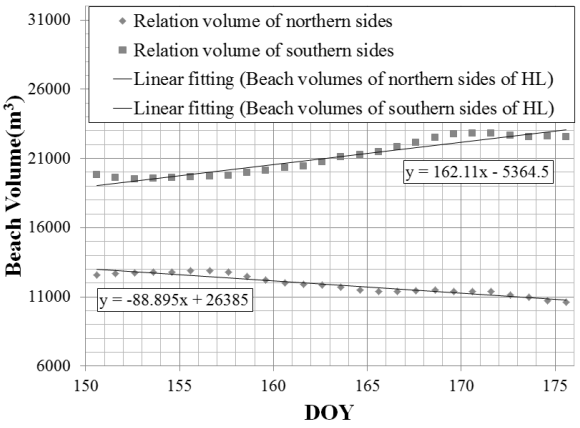

Fig.10 Variation graph of volume change for DOY 150 ~ 175

Comparison on Widths Surf Zone Between Radar and Computation

When estimate LSTR, widths of surfzone are important factors. Comparisons of widths of surfzone from radar images and from numerical model are carried out. Simple breaking index ($H > 0.78h$) is used in numerical model. Fig. 11 shows formations of surfzone from the numerical model. Comparisons of widths of surfzone between radar images and the numerical model are shown in Fig. 12.

Computation of LSTR with Numerical Model

Numerical models used in this study are REF/DIF-1 (Kirby et al.,1994) and SHORECIRC (Svendsen et al., 2000), which calculate wave deformation and variation of current respectively. Further, formula from Coastal Engineering Manual (2003) is used for LSTR formula estimation:

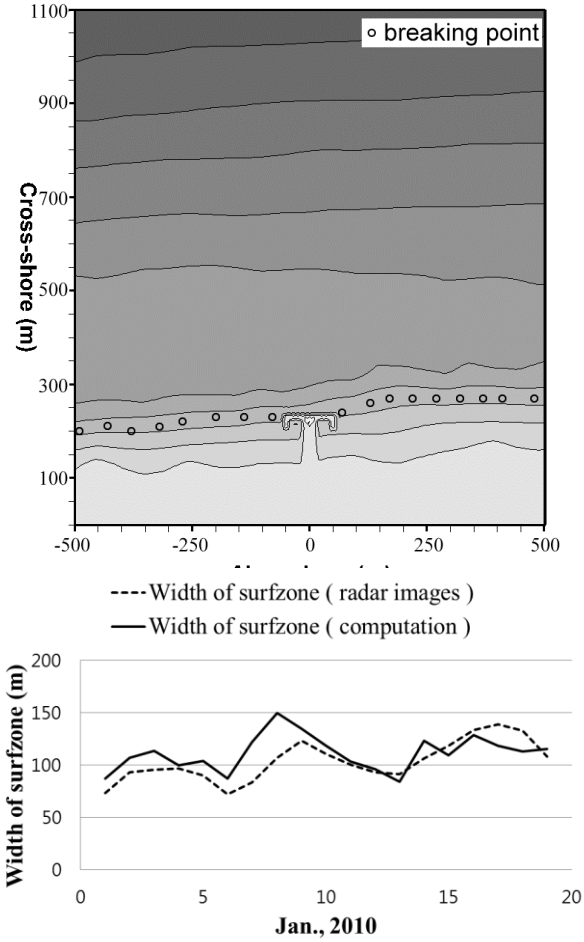

Fig.12 Comparison of widths of surfzone between radar images and numerical model

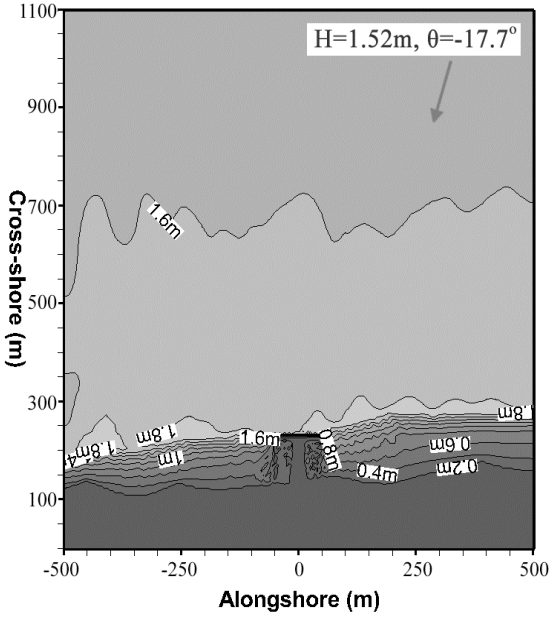

Fig.13 Result of computation on wave deformation

$$Q_l = \frac{K}{(\rho_s - \rho)g(1-n)} P_l \quad (1)$$

Here, Q_l is volume transport rate, n is porosity of sediment, and ρ_s and ρ are density of sand and water, respectively. K, proposed as 0.39 from Shore Protection Manual (1984), is a function of the breaker angle and ratio of the orbital velocity magnitude and the sediment speed and P_l is the breaking-wave-driven longshore energy flux and is defined as follows:

$$P_l = \frac{\rho g H_b W V_l C_f}{(5\pi/2)(V/V_o)_{LH}} \quad (2)$$

Table 1 Computational wave conditions for LSTR formula

Location (X)	W (m)	H_b (m)	V_l (m/sec)	Y (m)
-200 m	55	0.42	0.071	35
200m	75	0.57	0.096	45

In equation (2), ρ is density of water, g is acceleration of gravity, H_b is height of wave-breaking, W is width of surfzone, and V_l is longshore current velocity. C_f is bottom friction coefficient. $(V/V_o)_{LH}$ is theoretical dimensionless current velocity (Longuest-Higgins, 1970), and is defined as follows:

$$(\frac{V}{V_o})_{LH} = 0.2(\frac{Y}{W}) - 0.714(\frac{Y}{W})\ln(\frac{Y}{W}) \quad (3)$$

Where, Y is distance for the longshore current from the shore, $(V/V_o)_{LH}$ is assumed that the mixing parameter in Longuest-Higgins's theory is 0.4. V_o is theoretical longshore current velocity at breaking zone. V_l from numerical model at specific points are determined with Y. We decide on 35m and 45m at X= -200 m and 200m, respectively. We cannot use the same ratio of Y/W because of gird spacing (5 m) used in computation. So, we decide specific positions, with ration of Y/W = 0.64 and 0.6, according to approximations of $(V/V_o)_{LH}$ as the best alternative plan and approximations are $(V/V_o)_{LH} \approx 0.33$ at both X= -200 m and 200m. At these specific positions, longshore currents speeds from computations are substituted into V_l of equation (2). Variables introduced from computations for equation (2) and (3) are shown in Table 1. Value of the friction factor C_f in equation (2) was shown by Longuet-Higgins to be approximately 0.01, based on laboratory data.

The LSTR in this study are estimated as the following manner: After computations for the wave deformation by REF/DIF-1 model, current computations are carried out by SHORECIRC model. Surfzone width, breaking wave heights, and longshore current speed from the numerical computations are used for the estimation of LSTR with the formula described above.

Results of Numerical Computation

Wave conditions, averaged for the period of DOY 150~175 used in computation, are $H_{aver} = 1.52$m , $T_{aver} = 8.22$sec , and $\theta_{aver} = -17.7°$. Results of wave deformation and current filed are shown in Fig. 13 and 14. Variables needed in LSTR formula, surfzone width, breaking wave heights, and longshore current speed.

Comparison of the LSTR Estimation between Numerical Computation and Observation

Radar can only trace variations of the waterlines around the headland within intertidal zone. So, results of the LSTR from radar observation represent amounts of the littoral drift within the intertidal zone. On the other hands, results of the LSTR from numerical model represent amounts of the littoral drift within the whole surfzone from shore to wave-breaking line. Therefore, to compare results of the LSTR estimation of numerical model and observation, numerical computations are modified with the concept as shown in Fig. 15.

In Fig. 15, d_{total} is distance from shore to surfzone, d_{shore} is distance from shore to the intertidal zone, and Q_{total} and Q_{shore} are LSTR within whole surfzone and within the intertidal zone, respectively. Therefore, Q_{shore} is estimated from linear distribution as

$Q_{shore} = Q_{total}(d_{shore}/d_{total})$, and comparisons of the LSTR for northern and southern side of the headland are shown in Table. 2.

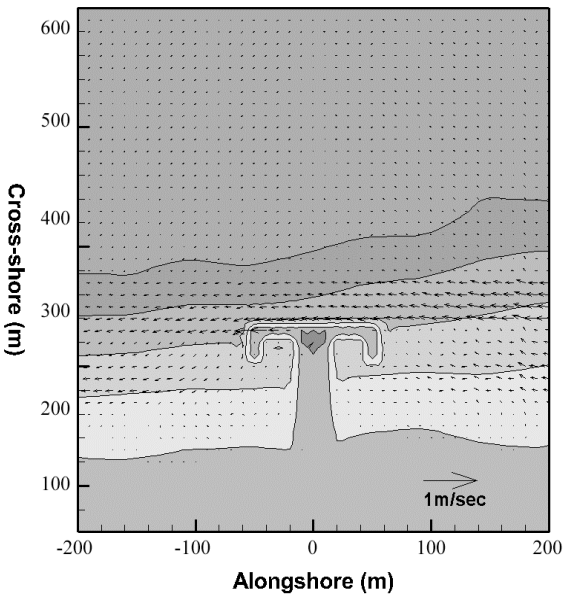

Fig.14 Result of numerical computation on current field

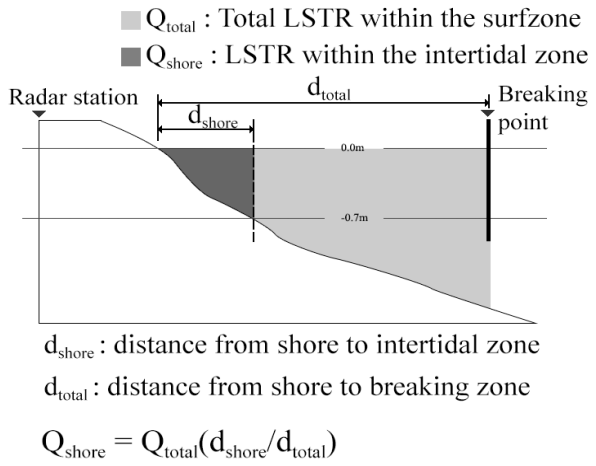

Table 2 Comparison of the LSTR between observation and computation

Fig.15 Estimation of the LSTR for intertidal zone

Location	Observation (m^3/day)	Computation (m^3/day)
Northern side	-89	-126
Southern side	-162	-172

The amount of LSTR differ 30% at northern side and around 9% at southern side of the headland between numerical computations and observations. Major factors of the difference may be that averaged wave conditions are used in numerical simulations but wave heights and directions varied during the period. To improve the estimation of LSTR, Consideration of fluctuation of wave conditions during the period.

REMARKS & FUTURE WORKS

Remarks

In this study, to estimate the LSTR with the numerical model, variations of distributions of the waterline are traced by X-band radar, and annual variations of the shoreline position and beach volumes are calculated. The LSTR from the numerical model are quantitatively compared with the LSTR from radar measurement.

Future works

In the future, to estimate the LSTR more exactly, upcoming main topics are as follows:

1. Consideration on the numerical simulation with detailed and not an averaged wave data.
2. Comparisons on the LSTR with short intervals yearly.
3. Consideration on the bathymetric change caused by current field in the numerical simulations.

REFERENCES

Coastal Engineering Manual (2003). Longshore sediment transport, part 3-2, Department of the ARMY US Army Corps of Engineers, Washington, Dc.

Kirby J.T, Dalrymple R.A, and Shi F. (1994). REF/DIF 1 Version 3.0, Center for Applied Coastal Research Department of Civil and Environmental Engineering University of Delaware, Res. NO. CACR-02-02.

Longuest-Higgins, M. S. (1970). Longshore currents generated by obliquely incident sew waves, part1 and 2, Journal of Geophysical Research, 75(33):6778-6801.

Shore Protection Manual (1984). Department of the ARMY US Army Corps of Engineers, Washington, Dc.

Svendsen I.A, Haas K., and Zhao Q. (2000). Quasi-3D Nearshore Circulation Model SHORECIRC Version 2.0, Center for Applied Coastal Research University of Delaware.

Takewaka S. (2005). Measurements of Shoreline Positions and Intertidal Foreshore Slopes with X-BAND Marine Radar System. Coastal Engineering Journal. 47(2-3) 91-107.